



## RESEARCH ARTICLE

10.1029/2018JA025454

## Energetic Particle Showers Over Mars from Comet C/2013 A1 Siding Spring

## Key Points:

- Both MAVEN and Mars Odyssey saw high-energy O<sup>+</sup> ions from comet Siding Spring
- The O<sup>+</sup> cometary ions deposited significant energy into the upper atmosphere
- Some effects may have persisted even after Mars left the outer coma of the comet

Beatriz Sánchez – Cano<sup>1</sup> , Olivier Witasse<sup>2</sup> , Mark Lester<sup>1</sup> , Ali Rahmati<sup>3</sup> , Richard Ambrosi<sup>1</sup>, Robert Lillis<sup>3</sup> , François Leblanc<sup>4</sup> , Pierre-Louis Blelly<sup>5</sup> , Marc Costa<sup>6</sup>, Stanley W. H. Cowley<sup>1</sup> , Jared R. Espley<sup>7</sup> , Stephen E. Milan<sup>1</sup> , Jeffrey J. Plaut<sup>8</sup> , Christina Lee<sup>3</sup> , and Davin Larson<sup>3</sup>

<sup>1</sup>Radio and Space Plasma Physics Group, Department of Physics and Astronomy, University of Leicester, Leicester, UK,

<sup>2</sup>European Space Agency, ESTEC-Scientific Support Office, Keplerlaan 1, Noordwijk, Netherlands, <sup>3</sup>Space Sciences

Laboratory, University of California, Berkeley, CA, USA, <sup>4</sup>LATMOS/IPSL, UPMC University Paris 06 Sorbonne Universités,

UVSQ, CNRS, Paris, France, <sup>5</sup>Institut de Recherche en Astrophysique et Planétologie, Toulouse, France, <sup>6</sup>European Space

Agency, ESAC, Villanueva de la Cañada, Madrid, Spain, <sup>7</sup>NASA Goddard Space Flight Center, Greenbelt, MD, USA, <sup>8</sup>Jet

Propulsion Laboratory, Pasadena, CA, USA

## Correspondence to:

B. Sánchez-Cano,  
bscmdr1@leicester.ac.uk

## Citation:

Sánchez – Cano, B., Witasse, O., Lester, M., Rahmati, A., Ambrosi, R., Lillis, R., et al. (2018). Energetic particle showers over Mars from comet C/2013 A1 Siding Spring. *Journal of Geophysical Research: Space Physics*, 123. <https://doi.org/10.1029/2018JA025454>

Received 9 MAR 2018

Accepted 25 JUL 2018

Accepted article online 6 AUG 2018

**Abstract** This paper is a phenomenological description of multispacecraft observations of energetic particles caused by the close flyby of comet C/2013 A1 Siding Spring with Mars on 19 October 2014. This is the first time that cometary energetic particles have been observed at Mars. The Mars Atmosphere and Volatile Evolution (MAVEN)-solar energetic particle (SEP) and the Mars Odyssey-High Energy Neutron Detector (HEND) instruments recorded evidence of precipitating particles, which are likely O<sup>+</sup> pickup ions, during the ~10 hr that Mars was within the region of the comet's coma. O<sup>+</sup> pickup ions were also detected several hours after, although whether their origin is the comet or space weather is not conclusive. We discuss the possible origin of those particles and also the cause of an additional shower of energetic particles that HEND observed between 22 and 35 hr after the comet's closest approach, which may be related to dust impacts from the comet's dust tail. An O<sup>+</sup> pickup ion energy flux simulation is performed with representative solar wind and cometary conditions, together with a simulation of their energy deposition profile in the atmosphere of Mars. Results indicate that the O<sup>+</sup> pickup ion fluxes observed by SEP were deposited in the ionosphere around 105 to 120 km altitude, and they are compared with precomet flyby estimations of cometary pickup ions. The comet's flyby deposited a significant fluence of energetic particles into Mars' upper atmosphere, at a similar level to a large space weather event.

**Plain Language Summary** Comet Siding Spring is a comet from the Oort cloud (a spherical shell of cometary bodies far beyond the solar system) that made a single flyby through the inner solar system in October 2014. It passed very close to Mars on 19 October 2014, at only one third of the Earth-Moon distance. This is a unique event as a close encounter of this type with Mars is predicted to occur only once in 100,000 years. In this work, we analyze data from the Mars Atmosphere and Volatile Evolution (MAVEN) and the Mars Odyssey missions in order to understand how the Martian atmosphere reacts to such an unusual external event. This is done through the study of energetic particles from the comet. These particles are important as they constitute an energy input into Mars' atmosphere and are therefore useful for understanding atmospheric evolution and habitability. We have found several O<sup>+</sup> detections from the comet, while Mars was within the comet environment (during ~10 hr). Also, we discuss several other interesting features that occurred after the closest approach, which could be related to comet dust tail impacts between 22 and 35 hr after the comet's closest approach. In general, the comet deposited into Mars' upper atmosphere a similar level of energy to that of a large space weather storm.

## 1. Context and Motivation

On 19 October 2014 at 18:28 UT, the Oort cloud comet C/2013 A1 (hereinafter Siding Spring) made its closest approach (CA) to Mars at 138,000 km (41.4 Mars radii), a third of the Earth-Moon distance. The gaseous coma washed over Mars, and the red planet passed directly through the cometary debris stream, as visualized in Figure 1, and at Espley et al. (2015) and Wang et al. (2016). As a close encounter of this type with Mars is predicted to occur only once in 100,000 years, this is likely the only opportunity for measurements associated with planetary/cometary encounters. This unique event enables us to investigate the response of the

©2018. The Authors.

This is an open access article under the terms of the Creative Commons Attribution License, which permits use, distribution and reproduction in any medium, provided the original work is properly cited.

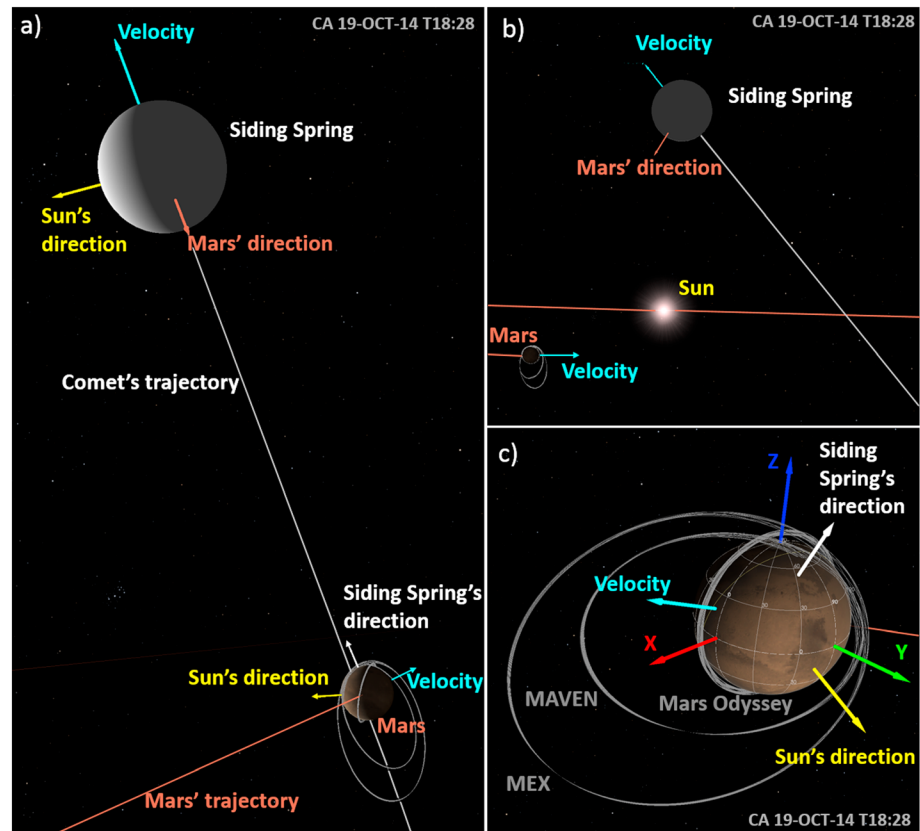


**Figure 1.** Geometry of the Mars-comet encounter at CA, created using the SPICE-enhanced tool Cosmographia. For a better visualization, comet Siding Spring has been represented as a sphere of radius 15,000 km. A 3-D visualization of the encounter can be found at <https://www.youtube.com/watch?v=dh18VxZX1dA>. (a) Side view of Mars and the comet, from the afternoon-dusk sector (the Sun is to the left). (b) View of the Sun, Mars, and the comet from behind Mars. (c) View of MAVEN, Mars Odyssey, and MEX orbit trajectories about Mars from near the comet's view. X, Y, and Z are the vector coordinates of Mars in a body fixed frame. MEX = Mars Express; CA = closest approach; MAVEN = Mars Atmosphere and Volatile Evolution.

Martian plasma system, as this may have implications for overall atmospheric evolution. However, before, during, and after the CA, there were significant space weather events, such as the impact of the flank of a large interplanetary coronal mass ejection (ICME) together with a corotating interaction region (CIR) ~44 hr prior to the CA (Lester et al., 2017; Witasse, Sánchez-Cano, Mays, et al., 2017) and a fast solar wind stream between 17 and 22 October, which make the interpretation of the observations challenging. The main goal of this work is to gain more knowledge about the energetic particle showers that rained over Mars during the comet Siding Spring flyby with the objective of determining the nature of the complex interaction between the solar wind during a highly active space weather interval, the comet, and Mars' upper atmosphere. To that end, a detailed phenomenological description from multispacecraft observations of the energetic particles that reached the Martian atmosphere, associated with the transit of comet Siding Spring, is presented. In this paper, we define energetic particles as charged particles and photons with energy in the range of kiloelectron volts up to ~2 MeV.

## 2. Previous Findings

Comet Siding Spring was discovered by Robert McNaught at the Siding Spring Observatory in Australia (McNaught et al., 2013) in 2013. It had a hyperbolic orbit with an inclination angle of 129° (heliocentric ecliptic J2000 reference) and moved from south to north of the ecliptic at the time of CA, traveling at a relative speed of ~56 km/s (JPL Small-Body Database; <https://ssd.jpl.nasa.gov/sbdb.cgi?>). Figure 1 shows the geometry of the encounter. When passing close to the Sun, ice sublimated from the surface, also releasing dust, and

producing a cometary spherical atmosphere called a *coma*, of which its outer part (outer coma) classically extends  $\sim 10^6$  km from the nucleus, and the inner and denser part (inner coma) typically extends  $\sim 10^5$  km (e.g., Cravens, 1997). Siding Spring is considered a dynamically new comet (Farnocchia et al., 2014) whose origin is found in the Oort cloud, and this is most likely its first passage through the solar system (Espley et al., 2015). Its water production rate at Mars was in situ and remotely estimated at  $1.1\text{--}1.5 \pm 0.5 \times 10^{28}$  molecules/s (Bodewits et al., 2015; Crismani et al., 2015; Schleicher et al., 2014), with a total impacting mass of gas at Mars of  $2.4 \pm 1.2 \times 10^4$  kg (Crismani et al., 2015). The dust activity of the coma was monitored for a year by Opatom et al. (2016) and Li et al. (2016) from telescopes observations, although there are no current estimates of the actual amount of dust deposited into the Martian atmosphere.

Mars transited the region of the outer coma of Siding Spring for  $\sim 10$  hr (Espley et al., 2015), which mainly affected the Martian southern hemisphere during the encounter (Wang et al., 2016), with a peak dust flux at  $\sim 20:06$  UT on 19 October (Tricarico et al., 2014) when Mars crossed the comet's orbital plane. As a result, dust particles ablated in the Martian ionosphere at 100 to 150 km altitude as measured  $\sim 5$  hr after CA, forming a strong ionization layer (Gurnett et al., 2015; Schneider et al., 2015), and a large increase in the total electron content (TEC) of the ionosphere (Restano et al., 2015). This cometary ionization layer was sustained for at least 19 hr after the dust peak flux on the nightside and 12 hr on the dayside (Venkateswara Rao et al., 2016). Moreover, several species of heavy ions were observed by the Mars Atmosphere and Volatile Evolution (MAVEN) mission down to  $\sim 185$  km for 2.5 days after CA (Benna et al., 2015).

Siding Spring, like a typical comet, also had two tails that extended millions of kilometers, a dust tail formed by material from the surface and coma that was blown away due to solar radiation pressure, and follows the comet's orbit but lagged behind the extended Sun-comet vector; and an ion tail (also called a gas tail) that is oriented antisunward direction with a lag angle of a few degrees. The ion tail is formed of pickup ions that have joined the flow of the solar wind, adding mass to it and decelerating it. This produces a draping of the magnetic field to form the induced magnetotail (or induced comet magnetosphere; e.g., Cravens & Gombosi, 2004), inside of which the ion tail is found. Mars was mainly affected by the outer coma, the *head* of the cometary magnetosphere, and the dust tail of Siding Spring and passed very close to the expected location of the outer edge of the inner coma (Espley et al., 2015).

The comet-solar wind interaction depends mainly on four factors, that is, on the production rate and outflow velocity of the cometary gas (comet activity), on the solar wind plasma and magnetic field characteristics, on the Sun's photon radiation, and on certain comet composition parameters (such as ionization cross sections; McKenna-Lawlor, 1999). In terms of comet activity, and so, in terms of interaction region sizes, Siding Spring can be considered similar to other comets at the time they were visited by previous missions, such as comets 21P/Giacobini-Zinner, 19P/Borrelly, 81P/Wild, 103P/Hartley2, and 67P/Churyumov-Gerasimenko (when at its perihelion). On the other hand, Siding Spring was about an order of magnitude more active than comets 26P/Grigg-Skjellerup, 9P/Tempel1, and comet 67P/Churyumov-Gerasimenko (before and after perihelion), and an order of magnitude less active than comet P/Halley (e.g., A'Hearn et al., 1995; Gicquel et al., 2012; Hansen et al., 2016; Huddleston et al., 1990; Johnstone et al., 1993; Mäkinen et al., 2001; McFadden et al., 1987; Meech et al., 2011). In terms of solar wind and solar radiation factors, each comet is different as the comet interaction with the solar wind strongly depends on the in situ solar activity conditions. For example, cometary pickup ions became much more energetic at comet 67P/Churyumov-Gerasimenko when approaching the Sun (larger solar radiation) as measured by the Rosetta mission (Goldstein et al., 2015). Likewise, the flux of energetic particles, the flux of accelerated cometary water ions, and the densities of cold and hot plasmas increased significantly as a consequence of several CIRs and ICMEs that hit this comet (e.g., Edberg, Alho, et al., 2016; Edberg, Eriksson, et al., 2016; Witasse, Sánchez-Cano, Mays, et al., 2017). Another example is comet P/Grigg-Skjellerup that was partly embedded within a CIR when the Giotto spacecraft encountered it, and consequently, the encounter was marked by a high interplanetary magnetic field (IMF) and high background particle fluxes, very different solar wind conditions to when the comet P/Halley was encountered by the same mission (Kirsch et al., 1997; McKenna-Lawlor, 1999).

As a result of the Mars and Siding Spring interaction with the solar wind, neutral species of the comet's coma were ionized by extreme ultraviolet (EUV) photoionization, charge exchange, and electron impact ionization processes, creating mainly  $O^+$  ions that were picked up and energized by the electric fields in the solar wind.

Consequently, showers of cometary energetic particles rained over Mars predominantly on its dayside hemisphere. Additionally, Mars has an oxygen exosphere within which the pickup ion process happens at all times (e.g., Luhmann et al., 1992; Luhmann & Kozyra, 1991; Leblanc & Johnson, 2001; Fang et al., 2008; Curry et al., 2013; Wang et al., 2014; Rahmati et al., 2014, 2015, 2017). However, during the comet flyby, the exospheric O<sup>+</sup> pickup ions were overshadowed by the cometary ones as we analyze in this study, and as previously predicted by Gronoff et al. (2014) and Wang et al. (2016). Before the comet flyby, Gronoff et al. (2014) and Wang et al. (2016) performed two pickup O<sup>+</sup> ion simulations based on the Rahmati et al. (2014) model but with different upstream conditions. Gronoff et al. (2014) predicted that the O<sup>+</sup> pickup ion flux would increase of 2 orders of magnitude above 50 keV, while Wang et al. (2016) predicted an enhancement between 1 and 100 keV. Both pieces of work estimated the deposition altitude in the ionosphere at 110 km.

In this work, first, we describe observations of energetic particles from various instruments and spacecraft during the encounter, and second, we estimate the O<sup>+</sup> pickup ion flux using the same model as Gronoff et al. (2014) and Wang et al. (2016) and also the deposition altitude in the ionosphere of those particles, both based on current multispacecraft observations. The main science questions that this work tries to answer are: How do we characterize the interaction between a comet and a planetary atmosphere from the energetic particles/pickup ions point of view? And how large was the energetic particle shower at Mars that Siding Spring produced? This part of the Siding Spring comet interaction with Mars has not been analyzed so far with in situ data, and it is important because it constitutes a significant energy input into Mars' atmosphere, which is also essential to understand atmospheric evolution and, subsequently, the habitability of the red planet.

### 3. Observations

Figure 2 shows observations of relevant parameters recorded by the MAVEN and Mars Odyssey missions. Mars was affected by the comet's coma for ~10 hr (Espley et al., 2015). The coma does not have a sharp boundary because the density decreases gradually with distance. However, a vertical transparent yellow bar has been included in Figure 2 to indicate when Mars was at a distance of less than 10<sup>6</sup> km from the comet and, therefore, presumably in the outer coma region. The CA is marked with a vertical gray dashed line. As we describe in the following subsections, special attention is given to several energy/particle enhancement intervals detected by the MAVEN-solar energetic particle (SEP) instrument and by the Mars Odyssey-High Energy Neutron Detector (HEND) instrument, which are denoted with a capital letter in Figure 2. Since geometries are key to understanding the data sets, Figures 3 and 4 show the MAVEN-SEP instrument field-of-view (FOV) vector components, and the Mars Odyssey orbit trajectory (i.e., HEND location) respectively, both in the Mars-Solar-Orbital (MSO) coordinate system for the same intervals highlighted in Figure 2. The main objective of Figures 3 and 4 is to identify the positions of the energy/particle enhancements in Figure 2 over the planet and so the nature of the particles detected by the instruments (pickup ions, dust sputtering, etc.). We note that the term SEP throughout the paper refers to the solar energetic particle instrument, not to solar energetic particles themselves. Other MAVEN instruments capable of recording energetic particles, such as the Suprathermal and Thermal Ion Composition (STATIC) instrument are not used in this study because they were not operating during the CA in order to protect them from cometary debris impacts.

#### 3.1. MAVEN-SEP Observations

Figures 2a–2c show the ion differential flux spectra and the total ion fluxes integrated over 30–1,000 keV from the MAVEN-SEP instrument plotted versus time from 19 to 21 October inclusive. SEP is a solid-state telescopic detector designed to measure the flux of solar energetic particles. SEP consists of two sensors, SEP1 and SEP2, each containing two double ended telescopes, which are mounted perpendicular to one another and that are able to measure ions over the energy range ~20–6,000 keV (Larson et al., 2015). The total FOV of each detector is 42° × 31° (~3% of the full sky), with the front look directions labeled SEP1f and SEP2f (usually oriented 45° away from the Mars-Sun line), and the rear SEP1r and SEP2r (usually oriented 135° away from the Mars-Sun line; Lillis et al., 2016). Energetic oxygen pickup ions are normally observed in the sunward hemisphere with SEP1f and SEP2f. The incident energy of oxygen ions has to be >60 keV (Rahmati et al., 2015), although the detected energy by SEP is lower than 60 keV due to a pulse height defect (more detailed information in Larson et al., 2015). SEP1r and SEP2r data are not displayed in Figure 2 as they do not show any notable cometary features at the time of the encounter. In this paper we focus only on the

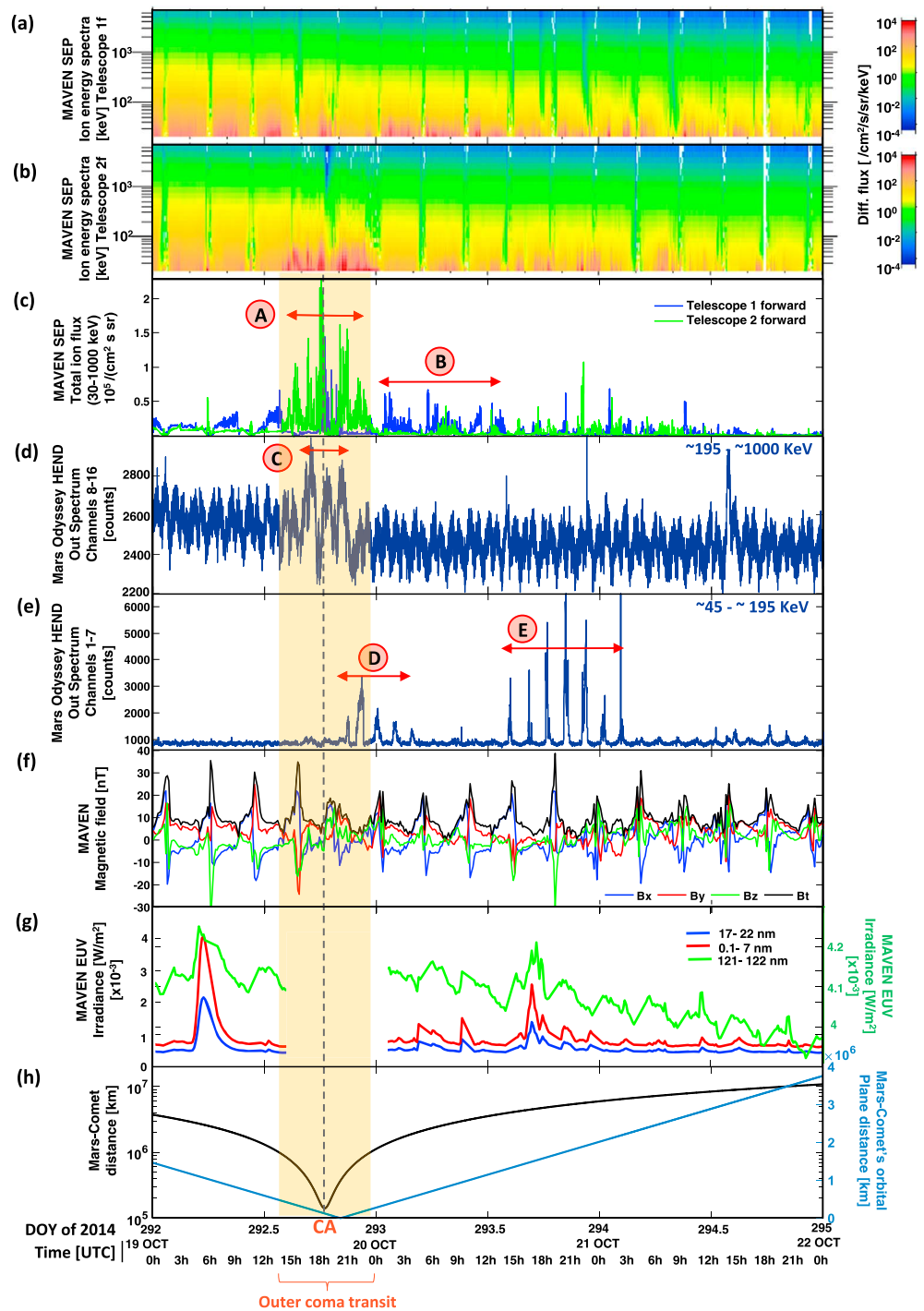


**Figure 2.** MAVEN and HEND observations as a function of time. In all panels, the Mars transit into the outer comet coma is marked with a yellow vertical band and the CA time with a vertical gray dashed line. The orbit geometry for the time periods denoted with a capital letter inside a red circle in panels (c)–(e) is shown in Figure 2. (a, b) MAVEN-SEP ion energy spectra of SEP1f and SEP2f, respectively. (c) MAVEN-SEP total ion flux of both SEP1f and SEP2f. (d) Mars Odyssey-HEND energy profiles from high-energy channels 8–16. (e) Same as in (d) but for lower-energy channels 1–7. (f) MAVEN-magnetometer observations. (g) MAVEN-EUV observations (only data with the Sun in the field of view). The red and blue profiles belong to the left ordinate axis and the green profile to the right one. (h) Mars-comet distance (black, left axis) and Mars-comet’s orbital plane distance (blue, right axis). MAVEN = Mars Atmosphere and Volatile EvolutionN; SEP = solar energetic particle; HEND = High Energy Neutron Detector; EUV = extreme ultraviolet; DOY = day of year.

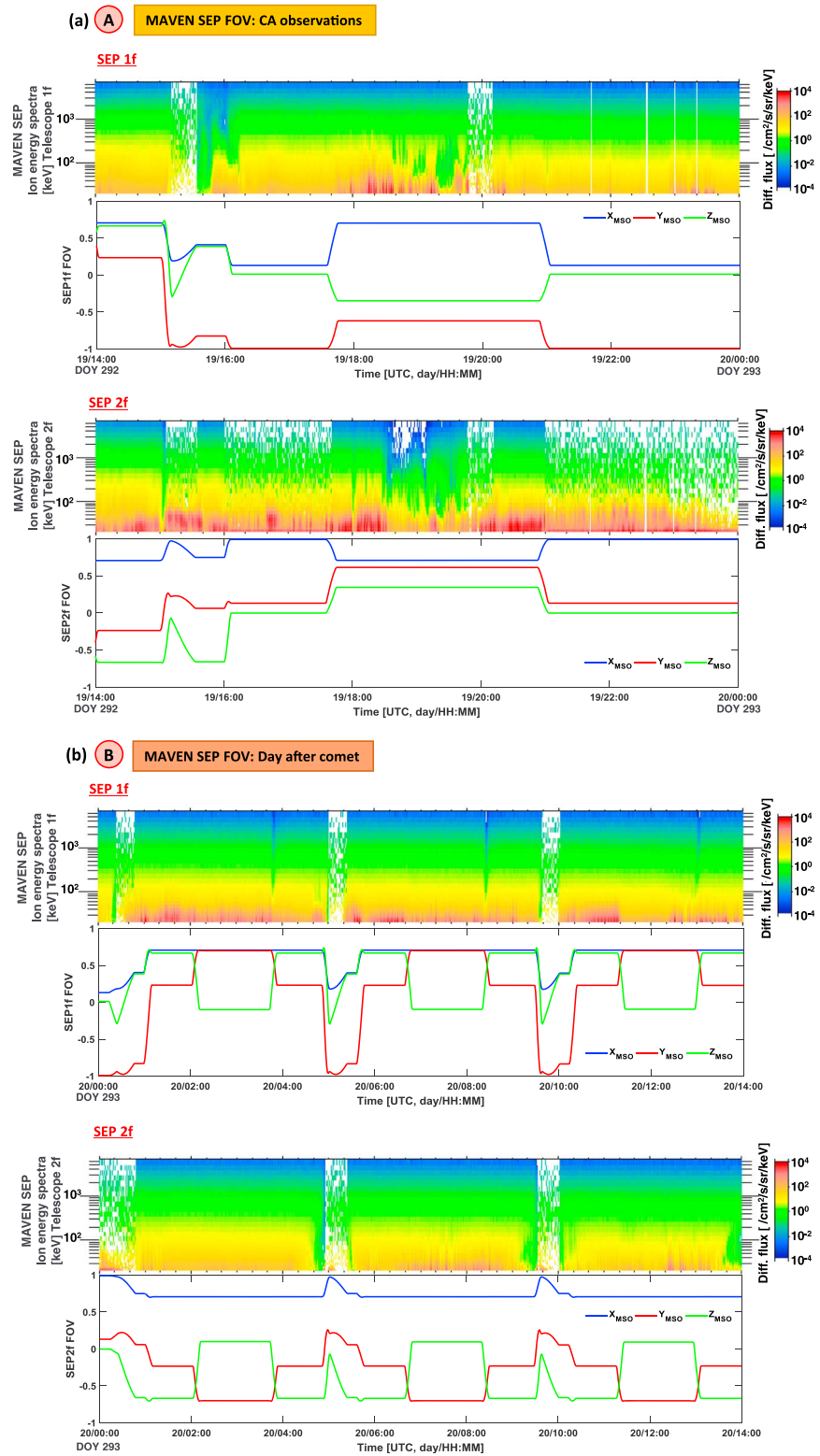


**Figure 3.** MAVEN-SEP geometry observations of both SEPf telescopes for the time periods denoted with a capital letter inside a red circle in Figure 2. (a) At the time of the CA (interval A), (b) a day after the comet flyby (interval B). For each telescope, the upper subpanel shows the MAVEN-SEPf Ion energy spectra (from Figure 2), and the bottom subpanel shows the FOV in Mars-Solar-Orbital coordinates. MAVEN = Mars Atmosphere and Volatile EvolutionN; SEP = solar energetic particle; FOV = field of view; CA = closest approach; DOY = day of year.

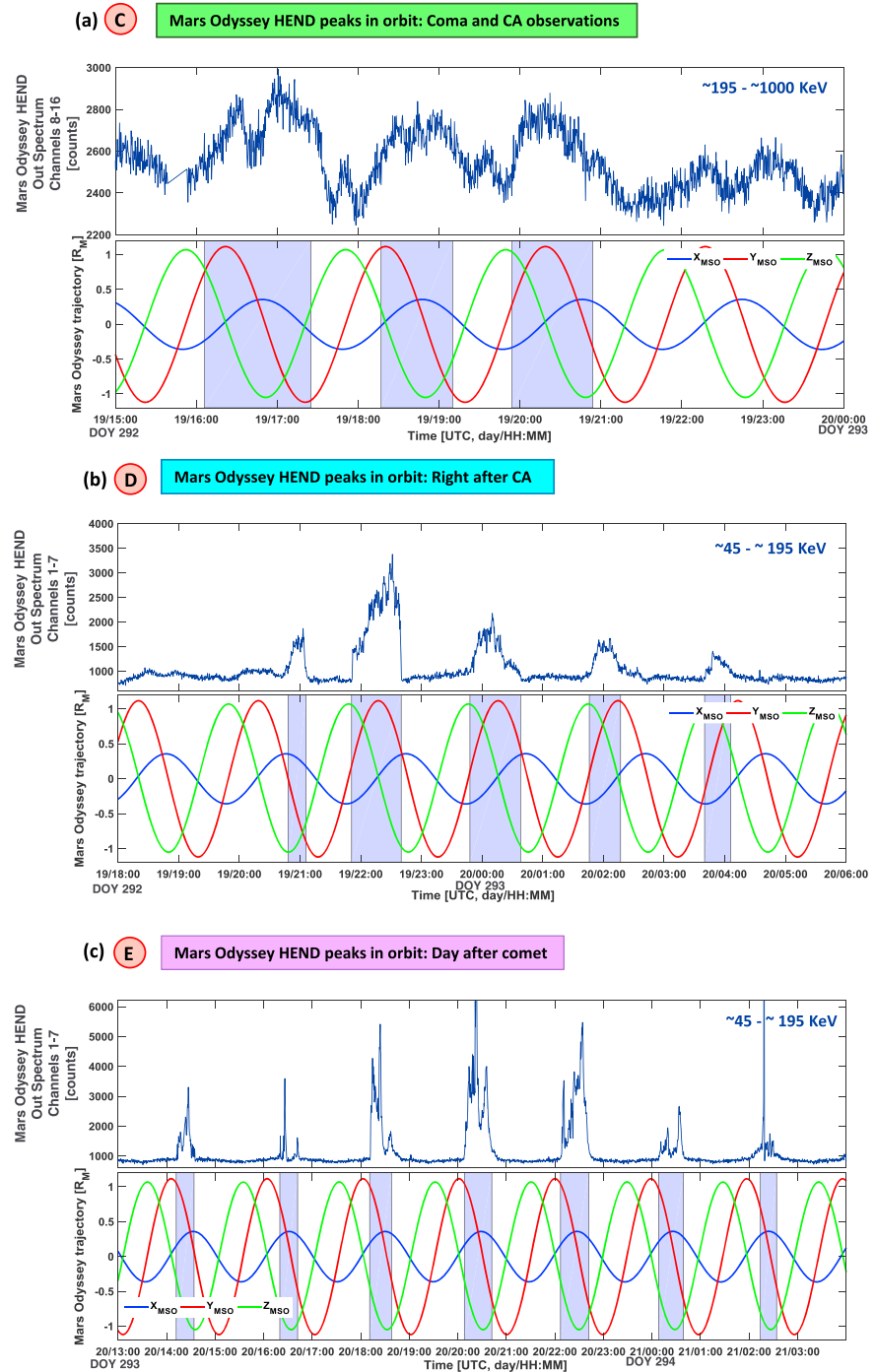


**Figure 4.** Mars Odyssey-HEND geometry observations for the time periods denoted with a capital letter inside a red circle in Figure 2. (a) At the time of the CA (interval C), (b) right after CA (interval D), and (c) a day after (interval E). In each panel, the upper subpanel shows the HEND observations (from Figure 2). The bottom subpanel shows the Mars Odyssey orbit in lines in Mars-Solar-Orbital coordinates. A colored square highlights the location of HEND enhancements. HEND = High Energy Neutron Detector; CA = closest approach; DOY = day of year.

period of the comet's encounter, but both the previous ICME and comet effects as recorded by the SEP instrument can be found in Figure A1 of the appendix or in Figure 6c of Witasse, Sánchez-Cano, Mays, et al. (2017). It is clear from visual inspection of Figures A1a–A1d that the SEP observations are notably

different before and after the comet encounter, even considering that, before the cometary encounter, a large ICME hit Mars. The SEP ion fluxes are quite variable immediately after the comet CA lasting for at least a couple of days, rather than immediately, as is the case after the ICME and fast stream transits. This suggests a very complex scenario of interactions between the comet and space weather event for several days (and not only for the CA time), as we discuss below.

The remnant effects of the ICME that hit Mars on 17 October are visible along the first three panels of Figure 2. The SEP background fluxes (blueish, greenish, and yellowish colors) gradually decrease in energy from 19 to 22 October, and there are several ion energy flux enhancements (reddish colors below  $\sim 50$  keV) before the comet flyby, which are most likely Mars exospheric pickup  $O^+$ . Despite this, the cometary effects recorded by MAVEN-SEP during the Mars transit of the comet's coma are clearly visible in the first three panels and are identified as interval A in Figure 2c (starting on 19 October 13:58 UT at  $9.1 \times 10^5$  km of distance to the comet before CA and ending on 20 October 00:31 UT at  $1.2 \times 10^6$  km of distance after CA). The prominent ion differential flux spectra (reddish colors) of SEP2f match almost perfectly with the time that Mars was at a distance of  $< 10^6$  km from the comet (yellow bar), with the maximum ion flux (SEP1f and SEP2f) at the time of CA. Although not shown here, energy fluxes also show a maximum at CA. This means that the assumption by Espley et al. (2015) of a coma radius of  $\sim 10^6$  km was realistic. These ion flux enhancements were detected between energies of  $\sim 30$  and  $\sim 100$  keV, being maximum at the lowest-energy levels and were detected on the dayside of both northern and southern Martian hemispheres (Figure 3a). These observations are qualitatively similar to the EPONA/Giotto observations at the CA of comet 26P/Grigg-Skjellerup in 1992 (McKenna-Lawlor & Afonin, 1999). In that case, the particle energy was  $\sim 60$ – $260$  keV, which is similar to our observations, taking into account the different flyby geometries (Giotto was only at  $\sim 200$  km from the comet's nucleus). The ideal case would be to obtain the actual pickup  $O^+$  flux and directions as a function of the energy, but due to the small SEP sky coverage, only a very small part of the pickup  $O^+$  ring-beam distribution is sampled, and we cannot determine the flux direction of all the incoming flux. Additionally, the disturbed background counts from the ICME passage and the fact that MAVEN was never in the solar wind during this period make the problem more complex. Nevertheless, observations during interval A seem consistent with  $O^+$  pickup ions from the comet's coma because of the timing of the observations and because SEP counts above  $\sim 50$  keV are 1–2 orders of magnitude above the level of counts for pickup  $O^+$  associated with the Martian hot oxygen exosphere (Rahmati et al., 2014). In spite of this, we note that there are other factors that can cause enhancements in SEP low-energy measurements to the level of saturation during solar disturbed conditions, as SEP has recorded during the last 3 years on Mars. For example, solar particle events associated with the passage of CIRs or ICMEs (e.g., Rahmati et al., 2017, and references therein). However, we recall that for this case, SEP observations look notably different before the CA than during and after CA (see Figure A1), even if there was a large ICME embedded within a CIR and followed by a long-lasting fast stream  $\sim 44$  hr before CA. Indeed, as Espley et al. (2015) indicated, Siding Spring produced effects in the magnetic field comparable to a large solar storm during CA, while here we view that this is the case also in terms of energetic particles. Smaller ion enhancements than at CA (up to  $\sim 60$  keV, reddish colors) were observed during the following 2 days (up to  $\sim 1 \times 10^7$  km of Mars-comet distance after CA), being more intense the day after CA up to  $\sim 4 \times 10^6$  km of Mars-comet distance (labeled B, Figure 2c) and more evident in the SEP1f detector. These signatures of interval B, again seen in the dayside of both hemispheres (Figure 3b), are most likely precipitating  $O^+$  pickup ions, although our analysis is not conclusive on whether these SEP detections are cometary  $O^+$  pickup ions or from Mars' exosphere. Simulations by Rahmati et al. (2014, 2015) show that in general  $O^+$  flux enhancements can only last up to an hour, not half a day after the source has disappeared. Therefore, another source must have been present to explain these pickup ion observations if they are from the comet. Since these signatures occurred only few hours after Mars' crossed the comet's orbital plane (Figure 2h, between  $3 \times 10^5$  and  $1 \times 10^6$  km after Mars crossed the comet's orbital plane) and, therefore, the denser part of the comet's tail, they could be related to less dense parts of the coma and dust tail hitting Mars. Additionally, these enhancements coincide with extraordinary magnetic turbulence in Mars' magnetosheath that lasted up to 20 October 09:00 UT (Espley et al., 2015), while the Mars' plasma system was recovering from the cometary encounter, which could help to understand the high variability of interval B. The solar wind disturbed conditions during the comet's flyby make difficult to draw a definitive conclusion on what was seen by the SEP detectors. There is the possibility that they were still related to the ICME's influence as previous studies have shown that extreme upstream solar wind conditions, such as ICMEs or fast solar wind periods can generate

these kinds of enhancements in SEP counts (Fang et al., 2013; Rahmati et al., 2015, 2017). However, we consider this scenario less probable for a number of reasons: first, the timing directly after the comet encounter; second, because as discussed before, it is obvious from Figure A1 that the observed SEP flux for a couple of days after the comet flyby is outstandingly different from the SEP flux after the ICME impact; third, because they occurred 3 days after the ICME onset and magnetic observations suggest that the Martian magnetosphere returned to nominal conditions after 30 hr (Espley et al., 2015); and fourth, because other instruments also detected possible cometary signals during this period as we now discuss.

### 3.2. Mars Odyssey-HEND Observations

Figures 2d and 2e show the HEND instrument measurements on board Mars Odyssey (Zeitlin et al., 2010). The HEND instrument is composed of five separate sensors that provide measurements of neutrons each one in a different energy range from 0.4 up to 15 MeV (Zeitlin et al., 2010). One of these sensors is the scintillator block (a neutron stilbene hydrocarbon spectrometer), which consists of two scintillators, an inner stilbene crystal surrounded by an outer cesium iodide (CsI (TI)) detector. Both scintillators are inside a light-tight housing of ~2-mm thickness (as seen from Figure 3 of Hurley et al., 2006), and both together have a sensitivity limit of ~2.5 MeV for high radiation fluxes. HEND records are somewhat more complex to evaluate than SEP because both scintillators are sensitive to neutrons, charged particles, and energetic photons (Livshits et al., 2005). As Livshits et al. (2005, 2006) and Hurley et al. (2006) describe, the energy intervals that both scintillators can record are 60 keV–2 MeV for the inner detector and 30 keV–1 MeV for the outer detector. The inner scintillator energy range includes radiation caused by the large number of electrons with energies ~100 keV, which produce gamma rays at the detector. The outer scintillator, which is a vetocounter and used for anticoincidence rejection of the outer charged particles (used for triangulation), is ideal for space weather analysis, as it is sensitive to minor to moderate solar particle events that hit the spacecraft and produce hard X-ray emissions. For both sensors, data are stored in 16 channels of growing energy starting from 0. In this study, we show data only from the outer scintillator, for which the approximate energy boundaries of each of its channels was calibrated by Livshits et al. (2017). Considering this calibration, the energy range of the channels plotted is ~195–>1,000 keV in Figure 2d and ~45–195 keV in Figure 2e.

In Figures 2d and 2e, peak-count enhancements were recorded in some parts of the Mars Odyssey orbit coinciding with the timing of the coma transit (intervals C in Figure 2d and D in Figure 2e). These types of short enhancements are commonly observed only in the lower channels of this data set in some periods of the year and, normally, are smaller in magnitude. Some of them are clearly associated with solar flares or solar energetic particle events, but the vast majority have an unknown origin. However, no other similar peak was observed from the beginning of September 2014 to 28 October 2014, with the exception of a single peak associated with the M1.1 solar flare produced on 14 October 2014 (Witasse, Sánchez-Cano, Mays, et al., 2017). The peaks in intervals C and D could be related to other solar flares that may have hit Mars during this period producing an enhanced X-ray flux at Mars, as the solar active region 12192 was the largest sunspot group observed in the last 24 years to that date and one of the most productive regions in terms of solar flares (Sun et al., 2015). However, we do not think this is the case because only small C-class flares occurred, while Mars was affected by the outer coma and whose timings do not match with the timing of any of the HEND peaks (see NOAA GOES XRS flare catalogue; <https://www.ngdc.noaa.gov/stp/space-weather/solar-data/solar-features/solar-flares/x-rays/goes/xrs/>). Moreover, a flare does not always produce a rise in HEND counts, for example, the MAVEN-EUV instrument detected an X1.1 flare on 19 October at 05:08 UT (Figure 2g; Peterson et al., 2016), but HEND did not show a response (Figures 2d and 2e). Previous studies of flare detections by HEND showed that the typical duration of a flare as recorded by this instrument is ~10–12 min, normally associated with photons with energy between 80 and 300 keV, having a sharp increase in counts, and are then followed by a slower decay. Moreover, a typical flare, if detected by HEND, does so independently of its position around the planet (see, e.g., Livshits et al., 2005; Livshits et al., 2006). We note that HEND's view of the Sun during this period was never obstructed by Mars, as the Sun was always in the FOV of Mars Odyssey throughout the Siding Spring encounter. Therefore, those HEND peaks identified as C and D were recorded in some preferential regions about the planet (Figures 4a–4b) and are well aligned with the comet flyby. Consequently for all these reasons, we consider that the HEND peaks in this study are not caused by solar flares.

Additionally, these peaks could be caused by a solar energetic particle event. However, this scenario is very unlikely to be the real cause: first, because a solar energetic particle event is normally associated with a flare or

an ICME, and in our case, both large flares and ICMEs occur well before these HEND observations; and second, because a solar energetic particle event normally lasts several days as recorded by HEND irrespective of where the spacecraft is in its orbit (e.g., Morgan et al., 2014). We note that in Witasse, Sánchez-Cano, Mays, et al. (2017), a complete solar wind simulation was presented in order to study the propagation of the ICME that hit Mars ~44 hr before the comet flyby. For that simulation, the full catalog of ICMEs for several months before and after this event was included. Considering this, we believe that there was no other ICME that affected Mars during this period. Likewise, we do not think that these peaks are due to neutrons recorded after a solar event, because in that case, a suppression in the count rate should have been seen, like the neutron count decrease observed during the transit of an ICME (the Forbush decrease; Forbush, 1938). For the ICME that hit Mars a day before the comet, we observed the final part of the Forbush decrease (decreasing flux trend) in Figure 2d. The minimum is reached at ~00:00 UT on 20 October (for more information see Witasse, Sánchez-Cano, Mays, et al., 2017, or Figure A1). We note that a Forbush decrease can be observed by neutron monitors in orbit around Mars and, also, by the radiation detector on board the Mars Science Laboratory (MSL) rover on Mars' surface. In the particular case of the Mars Odyssey orbiter, the HEND instrument can detect a full Forbush decrease if the ICME that produces the decrease does not have a very energetic SEP event associated to it. However, if the ICME has an associated energetic SEP, then, the neutron monitor does record it (e.g., as in Lawrence et al., 2016; Morgan et al., 2014). In our case, this means that the ICME that hit Mars on 17 October had some energetic particles traveling within it as MAVEN-SEP recorded, but those particles were not energetic enough to be recorded by HEND. Instead, HEND recorded a Forbush decrease. Peaks during interval C in Figure 2d were recorded, while the Forbush decrease was still occurring, and while Mars was transiting the comet's coma (inside the yellow bar, at less than  $10^6$  km from the comet). Therefore, we conclude that these HEND peaks are presumably photons, either as a result of gamma rays produced as secondary radiation after energetic coma particles hit the spacecraft (e.g., electrons or high-energy protons) and lose energy in the detector or as X-rays produced by electron bremsstrahlung after comet particles interact with the spacecraft and the instrument material. Another possibility is that these particles are ions from the coma, but in that case, they would need to be protons, which only need tens of mega electron volts to penetrate the instrument housing, or other energetic and heavier ions that penetrate directly from the entrance of the instrument (which is pointing toward the surface of Mars), and not from any other direction as they would need to be very energetic (approximately hundreds of mega electron volts) to be able to penetrate the housing of the detector and maybe even the spacecraft.

The peaks in interval C (starting on 19 October 16:06 UT at  $4.9 \times 10^5$  km from the comet before CA and ending on 19 October 20:54 UT at  $5.1 \times 10^5$  km from the comet after CA) lasted for intervals of ~1 hr on the almost 2 hr orbit and were recorded mainly in some of the higher energy channels (7–11, energy ~195–510 keV), mainly when Mars Odyssey was in the dayside and southern hemisphere of Mars (Figure 4a). Although not shown here, the inner detector also observed the same peaks on the same channels. Considering their location in relation to the comet position, they could be gamma ray photons originating from particles within the coma. Peaks in interval D (Figure 2e), which started on 19 October 20:48 UT at  $4.9 \times 10^5$  km from the comet after CA and ending on 20 October 04:06 UT at  $1.9 \times 10^6$  km from the comet, were registered mainly in channels 3–4 (energy ~86–132 keV) and with a duration of ~40 min on each consecutive orbit. They occurred directly after CA, and at the time when Mars crossed the comet's orbital plane (Figure 2h), that is, when Mars crossed the densest part of the dust tail. Furthermore, they lasted up to ~10 hr after Mars left the coma, being the first peak recorded on the dayside, south hemisphere and dawn-morning sector, and each consecutive peak gradually detected more at the nightside, north hemisphere and afternoon-dusk sector, which agrees with the comet trajectory in relation to Mars (Figure 4b). Although not shown here, the inner detector did not observe any of these peaks. Therefore, they could be hard X-ray photons produced by the impact of less energetic particles than for peaks in interval C. Because of the timing in relation to the comet flyby and the comet's orbital plane crossing, Mars location, and energy levels, these peaks could have originated from comet particles from localized peaks in the dust flux from the coma and the densest part of the dust tail. The peaks occur at the same time and in the same energy band as the enhancements in interval B as observed by SEP. They could also be cometary pickup ions, although accordingly to the Rahmati et al. (2014) model, these enhancements can hardly be associated with cometary  $O^+$  pickup ions as they would last only up to an hour (not up to 10 hr after the comet's flyby).

Finally, peaks in interval E in Figure 2e were visible mainly in the lowest-energy channels, 1–4 (energy ~45–132 keV) from 20 October 14:12 UT at  $4 \times 10^6$  km from the comet to 21 October 02:34 UT at  $6.5 \times 10^6$  km from

the comet ( $1 \times 10^6$ – $2.2 \times 10^6$  km from orbital plane crossing). Each peak lasted less than 30 min, and their origin is more enigmatic. These peaks occurred between 22 and 35 hr after CA and were recorded in seven consecutive Mars Odyssey orbits only in the area close to the Martian south polar cap, on the dayside and mainly on the afternoon-dusk hemispheres (Figure 4c). These observations are surprisingly very similar to an unexpected energetic ion detection by the EPONA instrument onboard the Giotto mission after the CA to the comet 26P/Grigg-Skjellerup in 1992 (McKenna-Lawlor & Afonin, 1999). The energetic ions were observed by the EPONA instrument in the energy range  $\sim 60$ – $100$  keV at  $9 \times 10^4$  km from the comet. Based on EPONA and magnetic field observations, McKenna-Lawlor and Afonin (1999) suggested that those late enhancements were caused by a fragment of the main comet within the comet's tail. This is because those late energetic ions were confined inside some magnetic boundaries that Giotto traversed. In our case, the energy range and location of the HEND observations from comet Siding Spring coincides very well with the EPONA observations, although it is not clear whether the peaks of interval E were caused by ions because of the HEND detector characteristics explained above. However, we note that during this period, SEP observed only small enhancements in ion fluxes (Figures 2a and 2b), with the exception of three short enhancements (Figure 2c) that coincide well with the last HEND peaks. As described before, the dust tail is formed because the solar radiation pressure blows material away from the comet's surface and coma and typically follows the comet's orbit. Although we did not find any telescope observations of the dust tail a day after the CA, theoretically, there is a possibility that the long dust tail affected Mars' plasma system while Mars was moving still *below* the comet (up to  $\sim 1$  day after CA), which moved from the south to the north of the ecliptic. If our hypothesis was correct, in part, this could also help to explain the persistent Martian ionospheric metallic layer for 2.5 days after CA (with a maximum 19 hr after the peak dust flux) observed by the Neutral Gas and Ion Mass Spectrometer (NGIMS) instrument on board MAVEN (Benna et al., 2015). The nature of the particles that produce the periodic peaks recorded by HEND in interval E are presently unknown, though with regard to timing and location in relation to the comet trajectory, they could be consistent with photons created by the impact of dust tail particles, as we discuss in the next section. However, we note that the HEND energy is higher than expected for heavy particles moving at 56 km/s, which is of the order of  $\sim 1$  MeV or less.

### 3.3. MAVEN-MAG and EUV Observations

In order to help with the interpretation of the peaks during interval E, magnetic field records from the MAVEN fluxgate magnetometers (MAG; Connerney et al., 2015) and EUV irradiance from the MAVEN EUV monitor (Eparvier et al., 2015) in the solar EUV wavelengths 0.1–7, 17–22, and 121.6 nm are plotted in Figures 2f and 2g, respectively. In these two panels, we focus our attention between 20 October 00:00 UT and 21 October 12:00 UT because a detailed assessment of the magnetic field observations during the comet encounter has already been carried out by Espley et al. (2015) and of the X1.1 flare observed in the EUV data on 19 October at 05:08 UT by Peterson et al. (2016). As Espley et al. (2015) described, there was significant turbulence in the magnetic field observations after CA and up to 20 October 9:00 UT. We consider that the subsequent orbits were relatively calm with maximum magnetic field magnitudes  $< 30$  nT at pericenter. However, on the following two orbits after 20 October 9:00 UT, MAG recorded a stronger and persistent negative Z-component of the magnetic field (always lower than for the ICME), whose magnitude seems unrelated to crustal fields (Cain et al., 2003; Morschhauser et al., 2014). These magnetic field observations could be related to a moderate density enhancement within the fast stream that was crossing Mars at that time (such as those discussed in Sánchez-Cano et al., 2017), as can be observed in the Mars Express solar wind measurements shown in Figures 6e and 6f of Witasse, Sánchez-Cano, Mays, et al. (2017).

The EUV instrument also recorded a large increase in its three wavelength bands at  $\sim 20$  October 18:00 UT that was caused by a M4.5 solar flare. It was preceded by two smaller increases between 20 October at 00:00 and 12:00 UT that were caused by a C9.0 and a M3.9 solar flare, respectively, and was succeeded by two smaller increases between 20 October 18:00 UT and 21 October that were caused by a M1.4 and a M1.7 solar flare, respectively (see NOAA GOES XRS flare catalogue). We note that the EUV observations from the 121.6-nm wavelength have a periodic oscillation (like a sawtooth pattern) with is related to MAVEN's orbit, as the 121.6-nm channel is sensitive to hydrogen in Mars' corona, which causes some of the structure. Further, the response function of this channel is more temperature dependent than the others and, therefore, is affected by temperature-induced variability along the orbit. Although these flares occurred at about the same period as the HEND peaks in interval E, the timing and magnitude of each single peak do not match

with the flare timing, the HEND peaks being greater in magnitude after the largest M-class flare during this period and lasting several hours longer than the last one. Moreover, as discussed before, this period was very intense in term of solar flares, but only the one that was ejected at the same time as the ICME caused a small enhancement in the HEND detector (e.g., see the null detection of the X1.1 flare at 05:08 UT on 19 October). Therefore, the origin of those peaks needs an alternative explanation.

A possible explanation could be X-rays originated by charge-exchange processes between the solar wind, Mars and the comet. This phenomenon is well known to occur at comets and planets when the solar wind encounters their neutral atmosphere (e.g., Bodewits et al., 2007; Dennerl, 2010). However, the X-rays emitted from this processes are typically much lower in energy ( $\sim < 1$  keV) than those recorded by HEND in this study. Considering that the peaks during interval E had a clear directionality and also were only registered by HEND, another possible explanation is that they were caused by a source of low-energy X-rays from a flaring galactic soft X-ray source that SEP's FOV did not see and that faded fairly quickly. Although possible, the energy related to this kind of source is typically lower than the energy registered by HEND. Another possible scenario is a magnetic connection between the comet and the spacecraft/Mars. Since Siding Spring was at a phase angle of  $\sim 90^\circ$  at that time, the Parker spiral would have to be very tightly wound and oriented out of the ecliptic for the IMF to connect to the vicinity of the comet's head. This would be very unusual, but not impossible as Gloeckler et al. (2004) found when the Ulysses mission observed two separate bursts of pickup ions downstream of comet C/1999 T1 McNaught-Hartley, caused by the passage of an ICME. The highly distorted field lines from the ICME ducted the cometary pickup ions over the Ulysses spacecraft. Those ions may have been streaming out of the comet and were detected during periods of magnetic connection between the comet and the spacecraft. Although possible, we consider that it is unlikely that direct reconnection could be doing some particle acceleration in our case. Unfortunately, the IMF orientation cannot be inferred from MAVEN-MAG because MAVEN was not placed in the undisturbed solar wind during this period.

After considering the MAG observations, the Mars Express moderate density enhancement in the solar wind (Witasse, Sánchez-Cano, Mays, et al., 2017, Figures 6e and 6f), the absence of positive detections of other peaks by HEND in about 2 months, the long-lasting enhancements in differential fluxes in SEP (reddish colors), and the location of those peaks in time and space (Figure 4c), the most realistic hypothesis is that the enhancements of interval E are a consequence of dust impact from the comet, as they are consistent with the comet's motion and with the dust traveling with it from the south to the north of the ecliptic, and from Mars's Keplerian leading hemisphere to the trailing hemisphere. Also, they occurred relatively very close to the comet's orbital plane ( $1\text{--}2.2 \times 10^6$  km of distance). The HEND peaks could have been created by electrons, protons, or photons produced by comet particles from the dust tail that hit the instrument. As commented in the previous subsection, observations from comet 26P/Grigg-Skjellerup by Giotto-EPONA seem to agree with this hypothesis (McKenna-Lawlor & Afonin, 1999). The specific link mechanism for these dust impacts is difficult to determine. A tentative scenario would be a dust population outside the comet's orbital plane that trails the comet in its path, such as described by, for example, Jenniskens et al. (2002). This is a well-known phenomenon that occurs with periodic comets, which experience slight variations in their trajectories leaving separate dust streams near their orbits. However Siding Spring may have been making its first journey through the inner solar system, and therefore, it is difficult to consider this explanation. Another possible explanation are slight variations of Siding Spring's orbital inclination that may have caused small changes on the comet's dust tail trajectory as nongravitational perturbations could significantly affect the comet trajectory, though this is not confirmed by the latest high precision comet trajectory estimates (Farnocchia et al., 2016) based on remote and in situ observations. Additionally, space weather activity could have enhanced any possible dust tail sputtering. A probable change in the IMF orientation toward a more negative  $B_z$  component within the fast stream, possibly together with dust material from the comet, could have enhanced any dust sputtering on the spacecraft.

#### 4. Pickup Ion Simulation and Energy Deposition in the Martian Atmosphere

Pickup ions can constitute an important source of heating and ionization at different altitudes in the Martian atmosphere depending on their kinetic energy (e.g., Fang et al., 2013; Leblanc, Modolo, et al., 2017; Luhmann & Kozyra, 1991). As described above, the pickup ion flux at Mars was greatly enhanced during and after the comet encounter, but it is necessary to distinguish whether their source is from Mars' hot exosphere or from Siding Spring. For that reason, we have performed a numerical simulation in order to determine a

**Table 1**  
Pickup Ion Simulation Results

Case number	Oxygen source	IMF in MSO coordinates (nT)	Omnidirectional flux ( $10^3 \text{ cm}^{-2} \text{ s}^{-1} \text{ keV}^{-1}$ ) For pickup ion energy of 30 keV	Omnidirectional flux ( $10^3 \text{ cm}^{-2} \text{ s}^{-1} \text{ keV}^{-1}$ ) For pickup ion energy of 50 keV	Omnidirectional flux ( $10^3 \text{ cm}^{-2} \text{ s}^{-1} \text{ keV}^{-1}$ ) For pickup ion energy of 100 keV	Omnidirectional total flux ( $10^5 \text{ cm}^{-2} \text{ s}$ )	Total energy flux ( $10^9 \text{ eV cm}^{-2} \text{ s}^{-1}$ )	Density of pickup $\text{O}^+$ Upstream of Mars ( $10^{-2} \text{ cm}^{-3}$ )
1	Siding Spring Mars	[0,+10,0]	1.9	2	2.5	4.0	36.5	0.50
2	Siding Spring Mars	[0,-10,0]	1.8	0.9	0.35	1.5	6.0	0.41
3	Siding Spring Mars	[+5,+5,0]	2	2.7	4	5.5	54.0	0.64
4	Siding Spring Mars	[+5,-5,0]	1.8	0.8	0.35	1.5	6.0	0.41
5	Siding Spring Mars	[-5,+5,0]	4.8	7		5.0	22.6	0.89
6	Siding Spring Mars	[-5,-5,0]	1.5	0.7		1.7	3.3	0.60
7	Siding Spring Mars	[+5,+2,-5]	3.5	5.5		3.9	18.9	0.65
			1.5	0.8		1.7	3.3	0.60
			3	4		3.0	13.9	0.54
			1.5	0.7		1.7	3.3	0.60
			6.5	10		7.6	37.3	1.22
			1.8	0.7		1.7	3.3	0.60
			11.2	18		14.4	73.0	2.36
			1.5	0.7		1.6	3.5	0.58

Note. Empty cells denote particles that are unable to be accelerated to this energy. MSO = Mars-Solar-Orbital; IMF = interplanetary magnetic field.

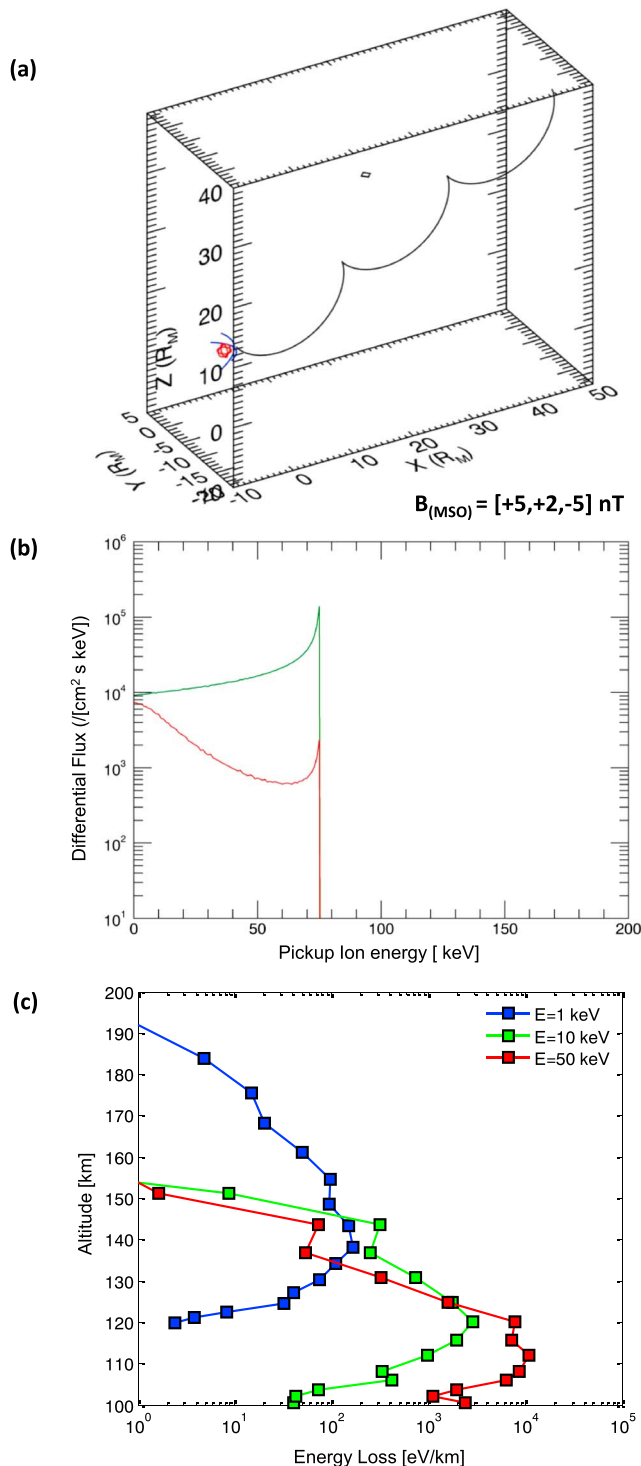


**Figure 5.** (a) Birth point of pickup ions reaching the sampling location for simulation case 7 (Table 1). Mars is in red, the bow shock in blue, and Siding Spring is a black diamond. (b) Omnidirectional differential flux of pickup  $O^+$  versus energy for Mars hot oxygen exosphere (red) and comet Siding Spring (green) for case 7. (c) Simulation of the energy loss for 1-, 10-, and 50-keV  $O^+$  test particles launched radially toward Mars at 300 km. MSO = Mars-Solar-Orbital.

better estimate of the cometary pickup  $O^+$  flux that reached Mars. The ideal situation would be to obtain the actual pickup  $O^+$  flux and directions from SEP, but due to its small sky coverage, this is not possible. Due to the distribution over Mars of the observations (Figure 3), this study is only focused on ions picked up in the less disturbed solar wind upstream of the bow shock which precipitate back to Mars' atmosphere. The simulation was run for the time of CA and was based on solar wind and comet observations, such as a comet water production rate of  $10^{28}$  molecule/s based on MAVEN observations (Crismani et al., 2015) and a solar wind speed of 650 km/s and a number density of  $5 \text{ cm}^{-3}$  based on Mars Express observations (Witasse, Sánchez-Cano, Mays, et al., 2017). The Mars hot oxygen exosphere model considered in the simulation is the one described by Rahmati et al. (2014) with the assumption of an isotropic neutral Martian exosphere. The neutral coma outflow speed was considered to be 1 km/s, the neutral species at Mars was assumed to be oxygen (mass 16 amu), and the oxygen ionization frequency was assumed to be  $5.10^{-7} \text{ s}^{-1}$  (obtained from photoionization, charge exchange, and electron impact ionization). As a reminder, the oxygen pickup ion gyroradii typically range between 5,000 and 50,000 km, depending on the solar wind velocity and the magnetic field vector. In the simulation, the pickup ion trajectories (three gyroperiods) were solved analytically, assuming uniform background fields (undisturbed solar wind conditions) and considering a pickup ion sampling location at 7,000-km radial distance from Mars' center, that is, upstream of the Mars nominal bow shock (e.g., Hall et al., 2016). The assumption of an undisturbed solar wind will probably no longer hold true because of the extreme space weather conditions of this period, though at least it provides an estimate of the  $O^+$  pickup ion flux just for the time of CA.

However, one of the key factors for the simulation is the direction and magnitude of the IMF, which can only be obtained from MAVEN as no other spacecraft at Mars carries a magnetometer. Unfortunately, MAVEN was far from the undisturbed solar wind, being always in the magnetosheath and upper atmosphere of Mars during this period. For that reason, we have performed seven simulations for different IMF scenarios. After considering both Mars' exosphere and the comet coma as oxygen sources, we present in Table 1 the results of the omnidirectional differential flux for different pickup ion energies (30, 50, and 100 keV) and the total flux, the total energy flux, and the total density of pickup  $O^+$  upstream of Mars for each of the seven simulations. To illustrate one simulation, Figure 5a shows the trajectory for case number 7,  $B$  (nT) = [+5, +2, -5] (in MSO coordinates), which is the one that the curve on which pickup ions are born passes closest to the comet at CA when compared to the other cases. In Figure 5a, the birth point of pickup ions reaching the sampling location are plotted. The corresponding omnidirectional differential flux of  $O^+$  pickup ions with respect to energy for the Mars hot oxygen exosphere (red) and comet Siding Spring (green) are shown in Figure 5b.

In general, the simulations are consistent in magnitude with the SEP observations (see Figures 2a and 2b). For the case of Mars' exosphere, in all seven cases, the larger the differential flux, the smaller the pickup ion energy. However, the differential flux level for the Siding Spring case according to the simulation is the opposite, being larger for higher energies, which provides evidence of a larger probability of delivering  $O^+$  pickup ions of cometary origin as also observed by SEP. The ratio of total energy flux between pickup ions originating from Mars and Siding

Spring is between 4 and 20 times higher for the comet, and the density of  $O^+$  upstream of Mars between 1 and 4 times. The largest fluxes and  $O^+$  densities, although not the largest energies, are predicted for case 7. However, larger pickup ion energies are predicted for cases 1 and 2, which would match better with the SEP observations at CA because SEP observed fluxes of the same order of magnitude for those energies (see Figures 2a and 2b). Precomet flyby estimations for active solar conditions by Gronoff et al. (2014) suggested a larger differential flux for larger energies, although we note that they showed fluxes only in the MSO-X direction, whereas the fluxes shown in this paper are omnidirectional.

To estimate the altitude at which the energy of these particles is deposited into the Martian atmosphere, we have performed a second simulation. The model used is the Exospheric Global Model (EGM) (Leblanc, Leclercq, et al., 2017; Leblanc, Modolo, et al., 2017) in which the trajectories of a few tens of thousands of test particles are simulated through Mars' atmosphere, as described by the Laboratoire de Météorologie Dynamique-Global Climate Model (LMD-GCM) (Chaufray et al., 2014; Gonzalez-Galindo et al., 2013). Each test particle is launched at 300-km altitude with a downward radial initial velocity with energy of 1, 10, and 50 keV. The thermosphere is taken to be composed of  $CO_2$ , CO, O,  $N_2$ , N, and Ar and corresponds to the solar longitude of the observations,  $L_s = 216.8^\circ$ . Only binary collisions are considered and are described using the Lewkow and Kharchenko (2014) scheme for collisions with less than 10 eV of relative energy and with the molecular dynamics scheme above allowing molecular dissociation and excitation (Leblanc & Johnson, 2002). An electronic loss term was also included following Johnson et al. (2000). The energy deposition profiles of vertically precipitating  $O^+$  particles within an atmospheric layer for the three different energies are displayed in Figure 5c. Each profile is the result of averaging over all latitudes and longitudes (from a  $30^\circ \times 60^\circ$  latitude/longitude grid) and the energy is decomposed into the energy lost by collisions with the different species considered in the LMD-GCM. The figure shows that for  $O^+$  particles with an energy of 1 keV, the deposition altitude is 140 km with a peak energy loss of  $\sim 100$  eV/km, for particles with 10 keV of energy, the altitude is  $\sim 120$  km and the peak energy loss  $\sim 1$  keV/km, and for particles with 50 keV, the altitude is 105–120 km with a peak energy loss of  $\sim 10$  keV/km. These profiles are important because these particles lose their energy when they precipitate into the Martian atmosphere, and, as a consequence, they might create extra heating and ionization, having some effects on the ionospheric profiles at different altitudes (e.g., Leblanc, Modolo, et al., 2017). For example, according to Fang et al. (2013), the heating rate close to the exobase of the atmosphere due to the precipitating particles at extreme solar wind conditions, such as after an ICME, could be significant compared to the EUV/ultraviolet solar flux. Wang et al. (2016) and Gronoff et al. (2014) [precomet flyby estimations] predicted a peak at 110 km, and Wang et al. (2016) estimated that the energy loss was  $\sim 10$  keV  $cm^{-3}/s$  for active solar conditions. Both predictions agree very well with the new results for  $O^+$  ions of 50 keV after in situ solar wind and cometary observations.

## 5. Concluding Remarks

We have analyzed multispacecraft observations of energetic particles caused by the close flyby of comet Siding Spring with Mars on 19 October 2014. This is the first time that energetic cometary particles have been observed in situ at Mars. We have identified different cometary effects:

1. Precipitating cometary  $O^+$  pickup ions on Mars' dayside during the  $\sim 10$  hr that Mars transited the comet's coma region (Mars at less than  $10^6$  km from the comet) were observed by the MAVEN-SEP instrument.
2. More  $O^+$  pickup ions on Mars' dayside were observed by SEP for several hours after CA, although whether its origin is from the comet cannot be firmly concluded. They could be related either to the coma and dust tail transits or to the extreme space weather activity.
3. Mars Odyssey-HEND instrument recorded flux enhancements during CA at energies of  $\sim 195$ –1,000 keV mainly on Mars' dayside and south hemisphere at  $\sim 5 \times 10^5$  km from the comet that could be produced by gamma photons created by electrons and energetic protons hitting the instrument from the coma region.
4. Also, HEND observed several flux enhancements at lower energies ( $\sim 45$ –195 keV) in both hemispheres and mainly in the dusk sector that seem consistent with X-ray photons created by coma and dust tail particles hitting the spacecraft as they occur when Mars crossed the comet's orbital plane few hours after CA.
5. Additionally, HEND observed a shower of energetic particles a day after CA, but only in the Martian southern hemisphere, near the polar cap, and on the dayside. We have discussed several possible origins, but the most probable source seems related to dust tail particles hitting the spacecraft.

6. The work has been completed with an  $O^+$  pickup ion energy flux simulation using the actual solar wind and cometary conditions, together with a simulation of the energy deposition profile in the atmosphere of Mars. Results indicate that the  $O^+$  pickup ion fluxes observed by SEP were deposited in the ionosphere around 105 to 120 km altitude. Future work will include an assessment of the effects of these particles on the ionosphere (Witasse, Sánchez-Cano, Molina-Cuberos, et al., 2017).
7. We conclude that despite the extreme solar wind conditions, the Siding Spring flyby of Mars produced effects comparable to a large solar storm in terms of energetic particle showers.

### Appendix A: Context for the Observations

In this section, we include an extended version (Figure A1) of some key observations plotted in Figure 2 that can help with the general understanding of the context of the comet's observations discussed in this work.

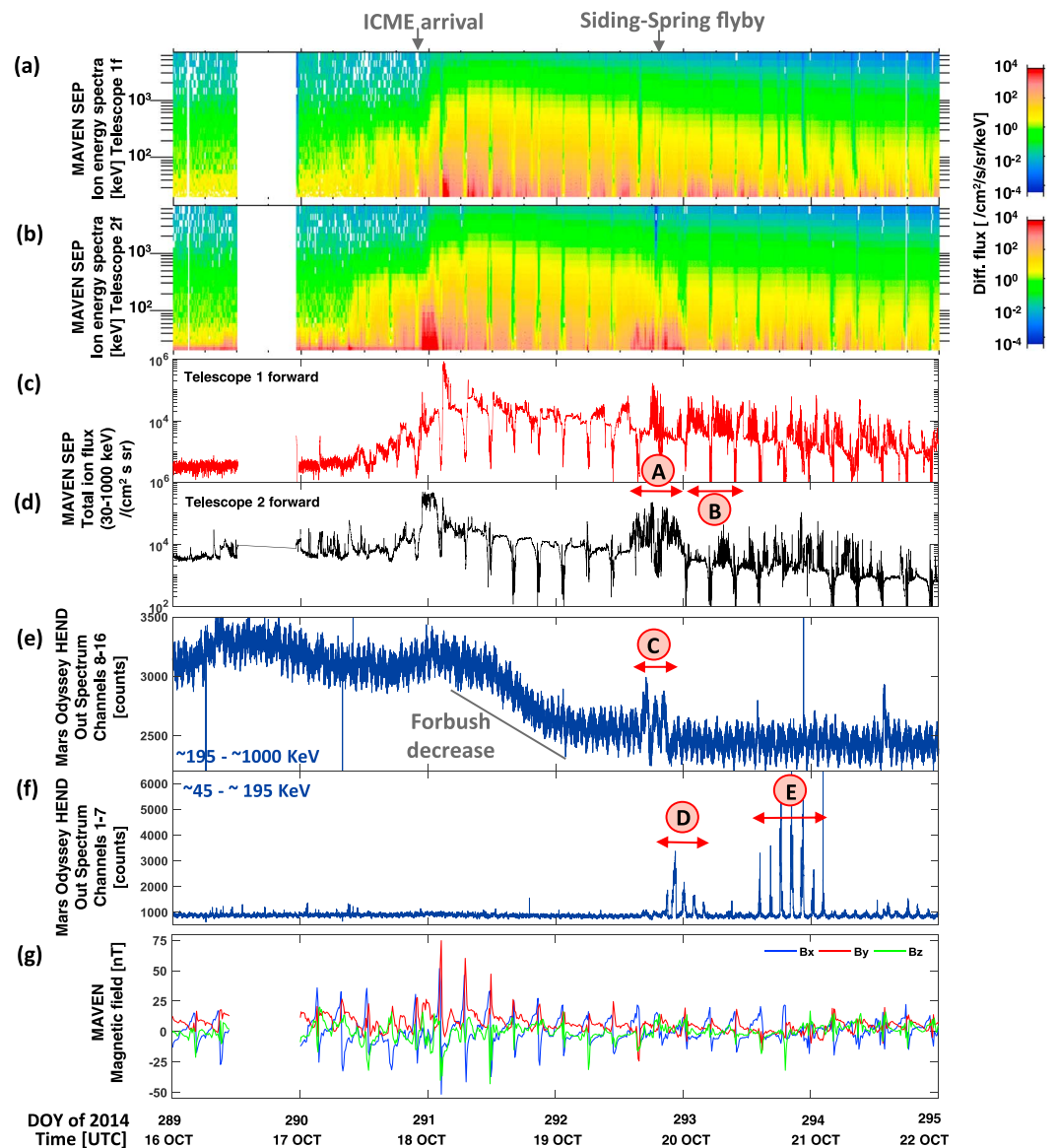


**Figure A1.** MAVEN and HEND observations as a function of time. (a, b) MAVEN-SEP ion energy spectra of SEP1f and SEP2f, respectively. (c, d) MAVEN-SEP total ion flux of SEP1f and SEP2f, respectively. (e) Mars Odyssey-HEND energy profiles from high-energy channels 8–16. (f) Same as in (e) but for lower-energy channels 1–7. (g) MAVEN-MAG observations in Mars-Solar-Orbital coordinates. ICME = interplanetary coronal mass ejection; MAVEN = Mars Atmosphere and Volatile Evolution; SEP = solar energetic particle; HEND = High Energy Neutron Detector; DOY = day of year.

For more detailed information of the ICME and space weather conditions we refer to Witasse, Sánchez-Cano, Mays, et al. (2017).

### Acknowledgments

B. S. -C., M. L., S. W. H. C., and S. E. M. acknowledge support through STFC grant ST/N000749/1. Authors acknowledge Jingnan Guo and Robert F. Wimmer-Schweingruber from Christian-Albrechts-University in Kiel (Germany), Ed Thiemann from University of Colorado (United States), and Jennifer Alyson Carter from University of Leicester (United Kingdom) for useful discussions. All data can be downloaded from the NASA PDS archive and from the MAVEN Science Data Center (<https://lasp.colorado.edu/maven/sdc/public/>). Part of the data analysis was performed with the help of the AMDA science analysis system provided by the Centre de Données de la Physique des Plasmas (CDPP) supported by CNRS, CNES, Observatoire de Paris, and Université Paul Sabatier, Toulouse. The latest trajectory of the comet can be found at [ftp://ssols01.esac.esa.int/pub/data/SPICE/MEX/kernels/spk/C2013A1\\_S105\\_MERGED.BSP](ftp://ssols01.esac.esa.int/pub/data/SPICE/MEX/kernels/spk/C2013A1_S105_MERGED.BSP); in addition, a web-based geometry service is available for the comet trajectory at [http://spice.esa.esa.int/webgeocalc/](http://spice.esac.esa.int/webgeocalc/), and a 3-D visualization of the encounter made with the SPICE-enhanced Cosmographia tool can be found at <https://www.youtube.com/watch?v=dh18VxZX1dA>. Support from the ESA-ESTEC Faculty is acknowledged. The authors would like to thank two anonymous reviewers for very constructive reviews that have helped to notably enhance the quality of this paper.

### References

- A'Hearn, M. F., Millis, R. L., Schleicher, D. G., Osip, D. J., & Birch, P. V. (1995). The ensemble properties of comets: Results from narrowband photometry of 85 comets, 1976–1992. *Icarus*, *118*(2), 223–270. <https://doi.org/10.1006/icar.1995.1190>
- Benna, M., Mahaffy, P. R., Grebowsky, J. M., Plane, J. M. C., Yelle, R. V., & Jakosky, B. M. (2015). Metallic ions in the upper atmosphere of Mars from the passage of comet C/2013 A1 (Siding Spring). *Geophysical Research Letters*, *42*, 4670–4675. <https://doi.org/10.1002/2015GL064159>
- Bodewits, D., Kelley, M. S. P., Li, J., Farnham, T. L., & A'Hearn, M. F. (2015). The pre-perihelion activity of dynamically new comet C/2013 A1 (Siding Spring) and its close encounter with Mars. *The Astrophysical Journal Letters*, *802*(1), L6. <https://doi.org/10.1088/2041-8205/802/1/L6>
- Bodewits, D., Christian, D. J., Torney, M., Dryer, M., Lisse, C. M., Dennerl, K., et al. (2007). Spectral analysis of the Chandra comet survey. *Astronomy & Astrophysics*, *469*(3), 1183–1195. <https://doi.org/10.1051/0004-6361:20077410>
- Cain, J. C., Ferguson, B. B., & Mozzoni, D. (2003). An  $n = 90$  internal potential function of the Martian crustal magnetic field. *Journal of Geophysical Research*, *108*(E2), 5008. <https://doi.org/10.1029/2000JE001487>
- Chaufray, J.-Y., Gonzalez-Galindo, F., Forget, F., Lopez-Valverde, M., Leblanc, F., Modolo, R., et al. (2014). 3D Martian ionosphere model: II. Effect of transport processes without magnetic field. *Journal of Geophysical Research: Planets*, *119*, 1614–1636. <https://doi.org/10.1002/2013JE004551>
- Connerney, J. E. P., Easley, J. R., DiBraccio, G. A., Gruesbeck, J. R., Oliverson, R. J., Mitchell, D. L., et al. (2015). First results of the MAVEN magnetic field investigation. *Geophysical Research Letters*, *42*, 8819–8827. <https://doi.org/10.1002/2015GL065366>
- Cravens, T. E. (1997). *Physics of solar system plasmas*. Cambridge, UK: Cambridge University Press. <https://doi.org/10.1017/CBO9780511529467>
- Cravens, T. E., & Gombosi, T. I. (2004). Cometary magnetospheres: A tutorial. *Advances in Space Research*, *33*(11), 1968–1976. <https://doi.org/10.1016/j.asr.2003.07.053>
- Crismani, M. M. J., Schneider, N. M., Deighan, J. I., Stewart, A. I. F., Combi, M., Chaffin, M. S., et al. (2015). Ultraviolet observations of the hydrogen coma of comet C/2013 A1 (Siding Spring) by MAVEN/IUVS. *Geophysical Research Letters*, *42*, 8803–8809. <https://doi.org/10.1002/2015GL065290>
- Curry, S. M., Liemohn, M., Fang, X., Ma, Y., & Easley, J. (2013). The influence of production mechanisms on pick-up ion loss at Mars. *Journal of Geophysical Research: Space Physics*, *118*, 554–569. <https://doi.org/10.1029/2012JA017665>
- Dennerl, K. (2010). Charge transfer reactions. *Space Science Reviews*, *157*(1–4), 57–91. <https://doi.org/10.1007/s11214-010-9720-5>
- Edberg, N. J. T., Alho, M., André, M., Andrews, D. J., Behar, E., Burch, J. L., et al. (2016). CME impact on comet 67P/Churyumov-Gerasimenko. *Monthly Notices of the Royal Astronomical Society*, *462*(Suppl 1), S45–S56. <https://doi.org/10.1093/mnras/stw2112>
- Edberg, N. J. T., Eriksson, A. I., Odelstad, E., Vigren, E., Andrews, D. J., Johansson, F., et al. (2016). Solar wind interaction with comet 67P: Impacts of corotating interaction regions. *Journal of Geophysical Research: Space Physics*, *121*, 949–965. <https://doi.org/10.1002/2015JA022147>
- Eparvier, F. G., Chamberlin, P. C., Woods, T. N., & Thiemann, E. M. B. (2015). The solar extreme ultraviolet monitor for MAVEN. *Space Science Reviews*, *195*(1–4), 293–301. <https://doi.org/10.1007/s11214-015-0195-2>
- Easley, J. R., DiBraccio, G. A., Connerney, J. E. P., Brain, D., Gruesbeck, J., Soobiah, Y., et al. (2015). A comet engulfs Mars: MAVEN observations of comet Siding Spring's influence on the Martian magnetosphere. *Geophysical Research Letters*, *42*, 8810–8818. <https://doi.org/10.1002/2015GL066300>
- Fang, X., Bougher, S. W., Johnson, R. E., Luhmann, J. G., Ma, Y., Wang, Y.-C., & Liemohn, M. W. (2013). The importance of pickup oxygen ion precipitation to the Mars upper atmosphere under extreme solar wind conditions. *Geophysical Research Letters*, *40*, 1922–1927. <https://doi.org/10.1002/grl.50415>
- Fang, X., Liemohn, M. W., Nagy, A. F., Ma, Y., De Zeeuw, D. L., Kozyra, J. U., & Zurbuchen, T. H. (2008). Pickup oxygen ion velocity space and spatial distribution around Mars. *Journal of Geophysical Research*, *113*, A02210. <https://doi.org/10.1029/2007JA012736>
- Farnocchia, D., Chesley, S., Chodas, P. W., Tricarico, P., Kelley, M. S. P., & Farnham, T. L. (2014). Trajectory analysis for the nucleus and dust of comet C/2013 A1 (Siding Spring). *The Astrophysical Journal*, *790*(2), 114. <https://doi.org/10.1088/0004-637X/790/2/114>
- Farnocchia, D., Chesley, S. R., Micheli, M., Delamere, W. A., Heyd, R. S., Tholen, D. J., et al. (2016). High precision comet trajectory estimates: The Mars flyby of C/2013 A1 (Siding Spring). *Icarus*, *266*, 279–287. <https://doi.org/10.1016/j.icarus.2015.10.035>
- Forbush, S. E. (1938). On world-wide changes in cosmic-ray intensity. *Physics Review*, *54*(12), 975–988. <https://doi.org/10.1103/PhysRev.54.975>
- Gicquel, A., Bockelée-Morvan, D., Zakharov, V. V., Kelley, M. S., Woodward, C. E., & Wooden, D. H. (2012). Investigation of dust and water ice in comet 9P/Tempel 1 from Spitzer observations of the Deep Impact event. *A&A*, *542*, A119. <https://doi.org/10.1051/0004-6361/201118718>
- Gloekler, G., Allegrini, F., Elliott, H. A., McComas, D. J., Schwadron, N. A., Geiss, J., et al. (2004). Cometary ions trapped in a coronal mass ejection. *The Astrophysical Journal*, *604*(2), L121–L124. <https://doi.org/10.1086/383524>
- Goldstein, R., Burch, J. L., Mokashi, P., Broiles, T., Mandt, K., Hanley, J., et al. (2015). The Rosetta Ion and Electron sensor (IES) measurement of the development of pickup ions from comet 67P/Churyumov-Gerasimenko. *Geophysical Research Letters*, *42*, 3093–3099. <https://doi.org/10.1002/2015GL063939>
- Gonzalez-Galindo, F., Chaufray, J. Y., Lopez-Valverde, M. A., Gilli, G., Forget, F., Leblanc, F., et al. (2013). Three-dimensional Martian ionosphere model: I. The photochemical ionosphere below 180 km. *Journal of Geophysical Research: Planets*, *118*, 2105–2123. <https://doi.org/10.1002/jgre.20150>
- Gronoff, G., Rahmati, A., Wedlund, C. S., Mertens, C. J., Cravens, T. E., & Kallio, E. (2014). The precipitation of keV energetic oxygen ions at Mars and their effects during the comet Siding Spring approach. *Geophysical Research Letters*, *41*, 4844–4850. <https://doi.org/10.1002/2014GL060902>
- Gurnett, D. A., Morgan, D. D., Persoon, A. M., Granroth, L. J., Kopf, A. J., Plaut, J. J., & Green, J. L. (2015). An ionized layer in the upper atmosphere of Mars caused by dust impacts from comet Siding Spring. *Geophysical Research Letters*, *42*, 4745–4751. <https://doi.org/10.1002/2015GL063726>
- Hall, B. E. S., Lester, M., Sánchez-Cano, B., Nichols, J. D., Andrews, D. J., Edberg, N. J. T., et al. (2016). Annual variations in the Martian bow shock location as observed by the Mars express mission. *Journal of Geophysical Research: Space Physics*, *121*, 11,474–11,494. <https://doi.org/10.1002/2016JA023316>
- Hansen, K. C., Altwegg, K., Berthelier, J. J., Bieler, A., Biver, N., Bockelée-Morvan, D., et al. (2016). Evolution of water production of 67P/Churyumov-Gerasimenko: An empirical model and a multi-instrument study. *Monthly Notices of the Royal Astronomical Society*, *462*, stw2413–S506. <https://doi.org/10.1093/mnras/stw2413>

- Huddleston, D. E., Johnstone, A. D., & Coates, A. J. (1990). Determination of the comet Halley gas emission characteristics from mass loading of the solar-wind. *Journal of Geophysical Research*, *95*(A1), 21–30. <https://doi.org/10.1029/JA095A01p00021>
- Hurley, K., Mitrofanov, I., Kozyrev, A., Litvak, M., Grinkov, A. S. V., Charyshnikov, S., et al. (2006). Mars Odyssey joins the third interplanetary network. *The Astrophysical Journal Supplement Series*, *164*(1), 124–129. <https://doi.org/10.1086/501352>
- Jenniskens, P., Lyytinen, E., de Lignie, M. C., Johannink, C., Jobse, K., Schievink, R., et al. (2002). Dust trails of 8P/Tuttle and the unusual outbursts of the Ursid shower. *Icarus*, *159*(1), 197–209. <https://doi.org/10.1006/icar.2002.6855>
- Johnson, R. E., Schnellenberger, D., & Wong, M. C. (2000). The sputtering of an oxygen thermosphere by energetic O<sup>+</sup>. *Journal of Geophysical Research*, *105*(E1), 1659–1670. <https://doi.org/10.1029/1999JE001058>
- Johnstone, A. D., Coates, A. J., Huddleston, D. E., Jockers, K., Wilken, B., et al. (1993). Observations of the solar wind and cometary ions during the encounter between Giotto and comet P/Grigg-Skjellerup. *A&A*, *273*(1), L1–L4.
- Kirsch, E., Daly, P. W., McKenna-Lawlor, S., Neubauer, F. M., & Coates, A. J. (1997). Observation of interplanetary particles in a corotating interaction region and of energetic water group ions from comet Grigg-Skjellerup. *Planetary and Space Science*, *45*(9), 1105–1117. [https://doi.org/10.1016/S0032-0633\(97\)00054-8](https://doi.org/10.1016/S0032-0633(97)00054-8)
- Larson, D., Lillis, R. J., Lee, C. O., Dunn, P. A., Hatch, K., Robinson, M., et al. (2015). The MAVEN solar energetic particle investigation. *Space Science Reviews*, *175*, 153–172. <https://doi.org/10.1007/s11214-015-0218-z>
- Lawrence, D. J., Peplowski, P. N., Feldman, W. C., Schwadron, N. A., & Spence, H. E. (2016). Galactic cosmic ray variations in the inner heliosphere from solar distances less than 0.5 AU: Measurements from the MESSENGER Neutron Spectrometer. *Journal of Geophysical Research: Space Physics*, *121*, 7398–7406. <https://doi.org/10.1002/2016JA022962>
- Leblanc, F., & Johnson, R. E. (2001). Sputtering of the Martian atmosphere by solar wind pick-up ions. *Planetary and Space Science*, *49*(6), 645–656. [https://doi.org/10.1016/S0032-0633\(01\)00003-4](https://doi.org/10.1016/S0032-0633(01)00003-4)
- Leblanc, F., & Johnson, R. E. (2002). Role of molecules in pick-up ion sputtering of the Martian atmosphere. *Journal of Geophysical Research*, *107*(E2), 1437. <https://doi.org/10.1029/2000JE001473>
- Leblanc, F., Leclercq, L., Oza, A., Schmidt, C., Modolo, R., Chaufray, J. Y., & Johnson, R. E. (2017). 3D multispecies collisional model of Ganymede's atmosphere. *Icarus*, *293*, 185–198. <https://doi.org/10.1016/j.icarus.2017.04.025>
- Leblanc, F., Modolo, R., Chaufray, J. Y., Leclercq, L., Curry, S., Luhmann, J., et al. (2017). On the origins of Mars' exospheric nonthermal oxygen component as observed by MAVEN and modeled by HELIOSARES. *Journal of Geophysical Research: Planets*, *122*, 2401–2428. <https://doi.org/10.1002/2017JE005336>
- Lester, M., Sanchez-Cano, B.; Witasse, O.; Mays, M. L. (2017). Space weather conditions before, during and after the comet Siding Spring encounter with Mars. EPSC Abstracts, Vol.11, EPSC2017-979, European Planetary Science Congress 2017.
- Lewkow, N. R., & Kharchenko, V. (2014). Precipitation of energetic neutral atoms and induced non-thermal escape fluxes from the Martian atmosphere. *Apl*, *790*(2), 98. <https://doi.org/10.1088/0004-637X/790/2/98>
- Li, J. Y., Samarasinha, N. H., Kelley, M. S. P., Farnham, T. L., Bodewits, D., Lisse, C. M., et al. (2016). *The Astrophysical Journal Letters*, *817*(2), L23. <https://doi.org/10.3847/2041-8205/817/2/L23>
- Lillis, R. J., Lee, C. O., Larson, D., Luhmann, J. G., Halekas, J. S., Connerney, J. E. P., & Jakosky, B. M. (2016). Shadowing and anisotropy of solar energetic ions at Mars measured by MAVEN during the March 2015 solar storm. *Journal of Geophysical Research: Space Physics*, *121*, 2818–2829. <https://doi.org/10.1002/2015JA022327>
- Livshits, M. A., Chernetskii, V. A., Bogomolov, A. V., Kuznetsov, S. N., Logachev, Y. I., Myagkova, I. N., et al. (2006). Stereoscopic observations of solar flares made onboard the 2001 Mars Odyssey spacecraft and CORONAS-F satellite. *Solar System Research*, *40*(2), 153–162. <https://doi.org/10.1134/S0038094606020092>
- Livshits, M. A., Chernetskii, V. A., Mitrofanov, I. G., et al. (2005). Hard X-ray and gamma-ray flares on the Sun: Stereoscopic effects near limb as observed by the *Odyssey* and near-Earth spacecraft. *Astronomicheskii Zhurnal*, *49*(11), 916–931.
- Livshits, M. A., Zimovets, I. V., Golovin, D. V., Nizamov, B. A., Vybornov, V. I., Mitrofanov, I. G., et al. (2017). Catalog of hard X-ray solar flares detected with Mars Odyssey/HEND from the Mars orbit in 2001–2016. *Astronomy Report*, *61*(9), 791–804. <https://doi.org/10.1134/S106372917090037>
- Luhmann, J. G., Johnson, R. E., & Zhang, M. H. G. (1992). Evolutionary impact of sputtering of the Martian atmosphere by O<sup>+</sup> pickup ions. *Geophysical Research Letters*, *19*(21), 2151–2154. <https://doi.org/10.1029/92GL02485>
- Luhmann, J. G., & Kozyra, J. U. (1991). Dayside pickup oxygen ion precipitation at Venus and Mars: Spatial distributions, energy deposition and consequences. *Journal of Geophysical Research*, *96*(A4), 5457–5467. <https://doi.org/10.1029/90JA01753>
- Mäkinen, J. T. T., Silén, J., Schmidt, W., Kyrölä, E., Summanen, T., Bertaux, J.-L., et al. (2001). Water production of comets 2P/Encke and 81P/Wild 2 derived from SWAN observations during the 1997 apparition. *Icarus*, *152*(2), 268–274. <https://doi.org/10.1006/icar.2001.6637>
- McFadden, L. A., A'Hearn, M. F., Feldman, P. D., Bohnhardt, H., Rahe, J., Festou, M. C., et al. (1987). Ultraviolet spectrophotometry of comet Giacobini-Zinner during the ICE encounter. *Icarus*, *69*(2), 329–337. [https://doi.org/10.1016/0019-1035\(87\)90109-6](https://doi.org/10.1016/0019-1035(87)90109-6)
- McKenna-Lawlor, S. (1999). Review, based on particles and fields observations made aboard the Giotto spacecraft concerning the nature of the solar wind interaction with comets P/Halley and P/Grigg-Skjellerup. *Space Science Reviews*, *88*, 501–528.
- McKenna-Lawlor, S., & Afonin, V. V. (1999). A flux enhancement measured in energetic particles ( $E \sim 60$ – $100$  keV) by the EPONA instrument aboard Giotto close to P/Grigg-Skjellerup, and its interpretation as the signature of a companion comet. *Planetary and Space Science*, *47*(3–4), 557–576. [https://doi.org/10.1016/S0032-0633\(98\)00137-8](https://doi.org/10.1016/S0032-0633(98)00137-8)
- McNaught, R. H., Sato, H., & Williams, G. V. (2013). Comet C/2013 A1 (Siding Spring). *Cent. Bureau Electr. Telegrams*, *3368*, 1.
- Meech, K. J., A'Hearn, M. F., Adams, J. A., Bacci, P., Bai, J., Barrera, L., et al. (2011). EPOXI: Comet 103P/Hartley 2 observations from a worldwide campaign. *The Astrophysical Journal Letters*, *734*(1), L1. <https://doi.org/10.1088/2041-8205/734/1/L1>
- Morgan, D. D., Diéval, C., Gurnett, D. A., Duru, F., Dubinin, E. M., Fränz, M., et al. (2014). Effects of a strong ICME on the Martian ionosphere as detected by Mars Express and Mars Odyssey. *Journal of Geophysical Research: Space Physics*, *119*, 5891–5908. <https://doi.org/10.1002/2013JA019522>
- Morschhauser, A., Lesur, V., & Grott, M. (2014). A spherical harmonic model of the lithospheric magnetic field of Mars. *Journal of Geophysical Research: Planets*, *119*, 1162–1188. <https://doi.org/10.1002/2013JE004555>
- Opitom, C., Guilbert-Lepoutre, A., Jehin, E., Manfroid, J., Hutsemékers, D., Gillon, M., et al. (2016). Long-term activity and outburst of comet C/2013A1 (Siding Spring) from narrow band photometry and long-slit spectroscopy. *Astronomy and Astrophysics*, *589*, A8. <https://doi.org/10.1051/0004-6361/201527628>
- Peterson, W. K., Thiemann, E. M. B., Eparvier, F. G., Andersson, L., Fowler, C. M., Larson, D., et al. (2016). Photoelectrons and solar ionizing radiation at Mars: Predictions versus MAVEN observations. *Journal of Geophysical Research: Space Physics*, *121*, 8859–8870. <https://doi.org/10.1002/2016JA022677>
- Rahmati, A., Cravens, T. E., Nagy, A. F., Fox, J. L., Bougher, S. W., Lillis, R. J., et al. (2014). Pickup ion measurements by MAVEN: A diagnostic of photochemical oxygen escape from Mars. *Geophysical Research Letters*, *41*, 4812–4818. <https://doi.org/10.1002/2014GL060289>

- Rahmati, A., Larson, D. E., Cravens, T. E., Lillis, R. J., Dunn, P. A., Halekas, J. S., et al. (2015). MAVEN insights into oxygen pickup ions at Mars. *Geophysical Research Letters*, *42*, 8870–8876. <https://doi.org/10.1002/2015GL065262>
- Rahmati, A., Larson, D. E., Cravens, T. E., Lillis, R. J., Halekas, J. S., McFadden, J. P., et al. (2017). MAVEN measured oxygen and hydrogen pickup ions: Probing the Martian exosphere and neutral escape. *Journal of Geophysical Research: Space Physics*, *122*, 3689–3706. <https://doi.org/10.1002/2016JA023371>
- Restano, M., Plaut, J. J., Campbell, B. A., Gim, Y., Nunes, D., Bernardini, F., et al. (2015). Effects of the passage of comet C/2013 A1 (Siding Spring) observed by the Shallow Radar (SHARAD) on Mars Reconnaissance Orbiter. *Geophysical Research Letters*, *42*, 4663–4669. <https://doi.org/10.1002/2015GL064150>
- Sánchez-Cano, B., Hall, B. E. S., Lester, M., Mays, M. L., Witasse, O., Ambrosi, R., et al. (2017). Mars plasma system response to solar wind disturbances during solar minimum. *Journal of Geophysical Research: Space Physics*, *122*, 6611–6634. <https://doi.org/10.1002/2016JA023587>
- Schleicher, D., Knight, M., & Skiff, B. (2014). Comet C/2013 A1 (Siding Spring). *Bureau Electronic Telegrams*, *4004*, 1.
- Schneider, N. M., Deighan, J. I., Stewart, A. I. F., McClintock, W. E., Jain, S. K., Chaffin, M. S., et al. (2015). MAVEN IUVS observations of the aftermath of the comet Siding Spring meteor shower on Mars. *Geophysical Research Letters*, *42*, 4755–4761. <https://doi.org/10.1002/2015GL063863>
- Sun, X., Bobra, M. G., Hoeksema, J. T., Liu, Y., Li, Y., Shen, C., et al. (2015). Why is the great solar active region 12192 flare-rich but CME-poor? *The Astrophysical Journal Letters*, *804*(2), L28. <https://doi.org/10.1088/2041-8205/804/2/L28>
- Tricarico, P., Samarasinha, N. H., Sykes, M. V., Li, J. Y., Farnham, T. L., Kelley, M. S. P., et al. (2014). Delivery of dust grains from comet C/2013 A1 (Siding Spring) to Mars. *The Astrophysical Journal Letters*, *787*(2), L35. <https://doi.org/10.1088/2041-8205/787/2/L35>
- Venkateswara Rao, N., ManasaMohana, P., Jayaraman, A., & Rao, S. V. B. (2016). Some new aspects of the transient ionization layer of comet Siding Spring origin in the Martian upper atmosphere. *Journal of Geophysical Research: Space Physics*, *121*, 3592–3602. <https://doi.org/10.1002/2015JA022189>
- Wang, Y.-C., Luhmann, J. G., Leblanc, F., Fang, X., Johnson, R. E., Ma, Y., et al. (2014). Modeling of the O<sup>+</sup> pickup ion sputtering efficiency dependence on solar wind conditions for the Martian atmosphere. *Journal of Geophysical Research: Planets*, *119*, 93–108. <https://doi.org/10.1002/2013JE004413>
- Wang, Y. C., Luhmann, J. G., Rahmati, A., Leblanc, F., Johnson, R. E., Cravens, T. E., & Ip, W. H. (2016). Cometary sputtering of the Martian atmosphere during the Siding Spring encounter. *Icarus*, *272*, 301–308. <https://doi.org/10.1016/j.icarus.2016.02.040>
- Witasse, O., Sánchez-Cano, B., Molina-Cuberos, G., Blelly, P.-L., Lester, M., Leblanc, F., et al. (2017). Comet Siding Spring's influence on the Mars' ionosphere. EPSC Abstracts, Vol.11, EPSC2017-131, European Planetary Science Congress 2017.
- Witasse, O., Sánchez-Cano, B., Mays, M. L., Kajdič, P., Opgenoorth, H., Elliott, H. A., et al. (2017). Interplanetary coronal mass ejection observed at STEREO-A, Mars.comet67P/Churyumov-Gerasimenko, Saturn, and New Horizons en route to Pluto: Comparison of its Forbush decreases at 1.4, 3.1, and 9.9 AU. *Journal of Geophysical Research: Space Physics*, *122*, 7865–7890. <https://doi.org/10.1002/2017JA023884>
- Zeitlin, C., Boynton, W., Mitrofanov, I., Hassler, D., Atwell, W., Cleghorn, T. F., et al. (2010). Mars Odyssey measurements of galactic cosmic rays and solar particles in Mars orbit, 2002–2008. *Space Weather*, *8*, S00E06. <https://doi.org/10.1029/2009SW000563>